Journal of Mathematics in Industry
a SpringerOpen Journal

RESEARCH Open Access

Theory and practice of micro water-oil displacement efficiency based on mathematical models

Haohan Liu[1,2*]

*Correspondence:
mittyliu123@outlook.com;
tsinghua616@163.com
[1]Sichuan College of Architectural Technology, Deyang, China
[2]Southwest Petroleum University, Chengdu, China

Abstract

Theoretical study about quantitative influence of the micro parameters (interfacial tension, wetting angle, distance, unit length, bottom radius, boundary distance, etc.) on the macro parameters (oil displacement efficiency, pressure gradient, etc.) in water-oil displacement process is very important. This paper focuses on the micro oil displacement efficiency calculation method in oil reservoir, building a new bridge between these parameters. Combining fluid motion equation, continuity equation to pressure gradient equation, the occurrence radius equation of remaining oil in different capillary is established; Taking mercury intrusion porosimetry experiment and constructing the mathematical model, new normal probability distribution of pore radius is achieved, and then a new probability function for injected water entering pore throat is established based on the occurrence radius equation and pore radius distribution equation; By using the Darcy's Law and definite integral theory, new micro oil displacement efficiency equation is obtained. The Nuclear Magnetic Resonance experiments show: new method gets high calculating accuracy, and can be used to guide oil reservoir development.

Keywords: Occurrence radius; Probability function; Definite integral theory; Oil displacement efficiency; Nuclear Magnetic Resonance experiment

1 Introduction

Experts and scholars focus on water-oil displacement efficiency for years. Richardson [1] shows the oil displacement efficiency in weak hydrophilic rock samples is higher than that in strong hydrophilic rock samples. And then, Morrow [2] find there is a negative correlation between the water-oil displacement efficiency and rock sample hydrophilic characteristics. Li [3] and He [4] study the Permeability influence on water-oil displacement efficiency in two different stages. Wang [5] gives the Positive correlation of feature value function and water-oil displacement efficiency. Cai [6] and Shen [7] and Chen [8] show the negative correlation of inhomogeneity of pore structure and water-oil displacement efficiency. Yu [9] studied the Oil and water viscosity ratio influence on water-oil displacement efficiency. Lu [10] studies the indication phenomenon is a key factor influence the oil displacement efficiency. Yan [11] gives that the water-oil displacement efficiency increased by Injection multiples. Jiao's research [12] shows that the EOR is logarithmic to the injected pore volume. Fu [13] shows the replacement pressure is positive correlative to

the oil displacement efficiency in the early development stage. Fan Li [14], Rogério Soares Silva [15], Zheng [16] and Dong [17] also work on how to improve the EOR. However, there is seldom theoretical research on micro factors influences (such as interfacial tension) on macro factors (oil displacement efficiency), and the explanation of oil field development phenomena is usually acted by our experiences.

In previous time, my team studied oil displacement efficiency from different aspects: based on the water flooding location, the water drive characteristic curve, the statistic methods ANN and $GM(1,n)$ and the time-varying system [18–24]. After years' study, we find there is a necessary quantitative connection between water-oil displacement efficiency and these micro factors. This manuscript aims to establish new relationships between macro parameter water-oil displacement efficiency, pressure gradient with the micro parameters interfacial tension, wetting angle, distance, unit length, bottom radius, boundary distance, etc. Then, we will get the interaction mechanism between the macro parameters and the micro parameters.

2 Remaining oil occurrence radius in capillary

For the incompressible single-phase liquid, the seepage process in a homogeneous reservoir is isothermal steady.

Fluid motion equation:

$$\overline{v} = \frac{K}{\mu}\nabla p. \tag{1}$$

Continuity equation:

$$\nabla \cdot \overline{v} = 0. \tag{2}$$

Combining Eq. (1) to Eq. (2), Eq. (3) is established:

$$\nabla^2 p = 0. \tag{3}$$

For some particular reservoir with bottom water or lumpy oil layer, etc, the liquid flow in the bottom well is spherical directed flow.

Using space polar coordinate form in Eq. (3), Eq. (4) is established:

$$R = \sqrt{x^2 + y^2 + z^2}. \tag{4}$$

Combing Eq. (4) to Eq. (3) gives:

$$\begin{aligned} &\frac{1}{R}\frac{d}{dR}\left(R\frac{dp}{dR}\right) = 0, \\ &\begin{cases} R = r_e, & p = p_e, \\ R = r_w, & p = p_w. \end{cases} \end{aligned} \tag{5}$$

By solving Eq. (5) gives Eq. (6) and Eq. (7):

$$p = p_e - \frac{p_e - p_w}{r_w^{-1} - r_e^{-1}}\left(R^{-1} - r_e^{-1}\right), \tag{6}$$

$$v = \frac{K}{\mu}\frac{p_e - p_w}{r_w^{-1} - r_e^{-1}}\frac{1}{R^2}. \tag{7}$$

For any stratigraphic micro unit, δ_R is the unit length, when the driving force in the place R is big enough to displace the crude oil in the pore throat, the Eq. (8) of pressure gradient is established:

$$\Delta p = |p_{R+\delta_R} - p_R| = \frac{p_e - p_w}{r_w^{-1} - r_e^{-1}}\frac{\delta_R}{R(R+\delta_R)}. \tag{8}$$

The pressure gradient in any pore throat in place R and $R + \delta_R$ equals to the overcoming resistance force, Eq. (9):

$$\Delta p = \frac{2\sigma}{r}|\cos\theta|. \tag{9}$$

Combing Eq. (8) to Eq. (9) gives the maximum occurrence radius equation of remaining oil in different capillary, see Eq. (10):

$$r_D = \frac{r_w^{-1} - r_e^{-1}}{p_e - p_w}\frac{2\sigma R(R+\delta_R)}{\delta_R}|\cos\theta|. \tag{10}$$

Hence, the maximum occurrence radius changed by pressure gradient $p_e - p_w$, wetting angle θ, the unit distance, the unit length δ_R^{-1}, the bottom radius r_w, the boundary distance r_e and the interfacial tension σ.

For polymer flooding, the polymerized substance can change the wetting angle and interfacial tension, and then the occurrence radius changed. By increasing displacement PV, the r_D will also be changed, we can also quantitatively compare the difference of water drive and polymer flooding efficiency with parameter r_D.

For heterogeneous oil reservoirs, the fluid motion equation and continuity equation will be changed, we can also use the above-mentioned steps to obtain r_D.

3 New oil displacement efficiency calculation method

The MIP experiment data show that the probability distribution of pore radius is normal. When using numerical fitting method, gives probability distribution equation of pore radius, Eq. (11):

$$\varphi(r) = C(r_{\max} - r)(r - r_{\min})e^{-\frac{(r-\overline{R})^2}{2\sigma_R^2}}. \tag{11}$$

For any capillary in the given unit length δ_R, the radius is r_i, the pore volume is:

$$V(r_i) = \pi r_i^2 \delta_R. \tag{12}$$

In the displacement process, the water first enters the large capillary pores, and then gradually enters the small capillary pores corresponding with the increase of pressure; for the imbibition process, the phenomenon is just reversed. Assume that the water can complete displace the oil in the capillary, and then we get the oil displacement efficiency $E_{D1}(r_D)$:

$$E_{D1}(r_D) = \frac{\sum_{i=1}^{m}\varphi(r_i)V(r_i)}{\sum_{j=1}^{n}\varphi(r_j)V(r_j)} = \frac{\sum_{i=1}^{m}\varphi(r_i)\pi r_i^2\delta_R}{\sum_{j=1}^{n}\varphi(r_j)\pi r_j^2\delta_R}. \tag{13}$$

Where i counts from 1 to the number of capillary in the interval $[r_D, r_{\max}]$, and j counts from 1 to the number of capillary in the interval $[r_{\min}, r_{\max}]$.

Introducing definite integral theory to Eq. (13), gives

$$E_{D1}(r_D) = \frac{\lim_{r_i \to 0} \sum_{i=1}^{m} \varphi(r_i)\pi r_i \delta_R(r_i)\Delta r_i}{\lim_{r_j \to 0} \sum_{j=1}^{n} \varphi(r_j)\pi r_j \delta_R(r_j)\Delta r_j} = \frac{\int_{r_D}^{r_{\max}} \varphi(r) r \delta_R(r)\, dr}{\int_{r_{\min}}^{r_{\max}} \varphi(r) r \delta_R(r)\, dr}. \tag{14}$$

When fixing the unit length in any capillary, it is

$$\delta_R(r) = \delta_R. \tag{15}$$

Combing Eq. (11), Eq. (15) to Eq. (14) gives

$$E_{D1}(r_D) = \frac{\int_{r_D}^{r_{\max}} r(r_{\max} - r)(r - r_{\min}) e^{-\frac{(r-\overline{R})^2}{2\sigma_R^2}}\, dr}{\int_{r_{\min}}^{r_{\max}} r(r_{\max} - r)(r - r_{\min}) e^{-\frac{(r-\overline{R})^2}{2\sigma_R^2}}\, dr}. \tag{16}$$

However, not all of the injected water enters the capillary pores, the residual part, the discontinuous part and the possible formation pathway should be taken into consideration. In order to get the probability function for injected water entering pore throat, the fluid conductivity function $\eta(r)$ should be established. According to the Poiseuille Law, the flow equation in single capillary can be established:

$$q = \frac{\pi r^4 \Delta p}{8\mu L}, \quad r_w \le L \le r_e. \tag{17}$$

The fluid conductivity function in single capillary is achieved:

$$\eta(r, L) = \frac{q}{\Delta p} = \frac{\pi r^4}{8\mu L}. \tag{18}$$

Hence, the probability function $J_k(r_D)$ is obtained

$$J(r_D) = \frac{\sum_{r_D \le r \le r_e} \eta(r)}{\sum_{r_{\min} \le r \le r_e} \eta(r)} = \frac{\int_{r_D}^{r_{\max}} r^3\, dr}{\int_{r_{\min}}^{r_{\max}} r^3\, dr} = \frac{(r_{\max})^4 - (r_D)^4}{(r_{\max})^4 - (r_{\min})^4}. \tag{19}$$

Hence, the oil displacement efficiency E_D can be calculated

$$\begin{aligned} E_D(r_D) &= J(r_D) E_{D1}(r_D) \\ &= \frac{(r_{\max})^4 - (r_D)^4}{(r_{\max})^4 - (r_{\min})^4} \frac{\int_{r_D}^{r_{\max}} r(r_{\max} - r)(r - r_{\min}) e^{-\frac{(r-\overline{R})^2}{2\sigma_R^2}}\, dr}{\int_{r_{\min}}^{r_{\max}} r(r_{\max} - r)(r - r_{\min}) e^{-\frac{(r-\overline{R})^2}{2\sigma_R^2}}\, dr}. \end{aligned} \tag{20}$$

Here, $E_D(r_D)$ is an error function, $E_D(r_D) = \mathrm{erf}(r_D)$, math software-Matlab can be used to calculate the numerical solution.

Figure 1 PIM experiment data figure

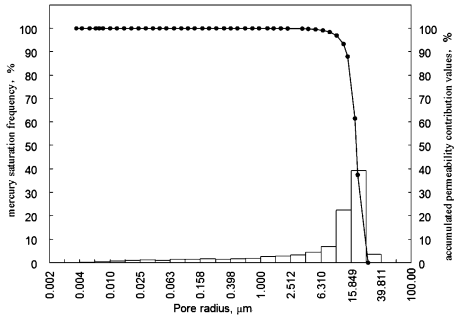

Figure 2 Normal distribution fitting curve

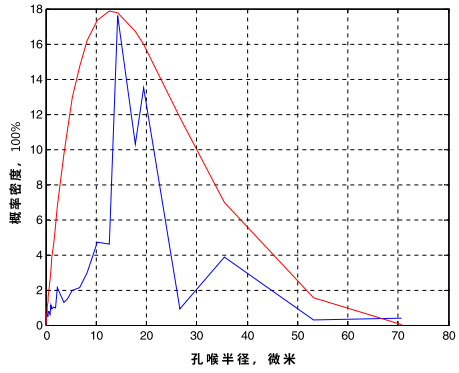

Table 1 Parameter values

$r_{\min}$, μm	$r_{\max}$, μm	δ_R, m	r_e, m	r_w, m	θ	σ	s_{wc}
70	2	0.1	300	0.2	$\frac{3}{4}\pi$	0.025 $\mathrm{N}\cdot\mathrm{m}^{-1}$	0.15

Hence, E_D is a function of $\Delta p, r_w, r_e, \sigma, \delta_R, \theta$, it is

$$E_D = E_D(r_D) = E_D(\Delta p, r_w, r_e, \sigma, \delta_R, \theta). \tag{21}$$

By introducing related reservoir engineering measurement to change related factors can lead to the change of E_D.

4 Results and discussion

(1) *PIM experiment and pore radius distribution*. By analyzing lots of PIM experiment data, we find the distribution of pore radius follows the normal distribution, such as the data from GD7-42-J195TG block of SL oilfield. The data figure between mercury saturation, accumulated permeability contribution values and pore radius is given, see Fig. 1.

By using the numerical fitting method, the normal distribution fitting equation is achieved, see Fig. 2:

$$\varphi(r) = 0.0478(r_{\max} - r)(r - r_{\min})e^{-0.0396r^{1.12}}. \tag{22}$$

(2) *Calculation of oil displacement efficiency*. The related parameter values in GD7-42-J195TG block see Table 1.

Figure 3 Occurrence radius in different well place

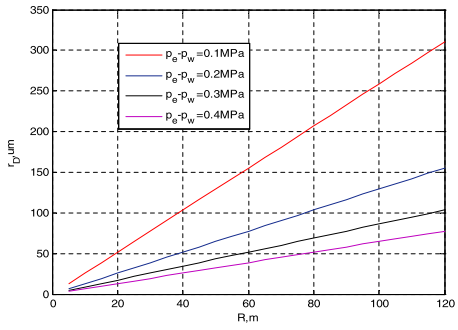

Figure 4 Occurrence radius in different pressure gradient

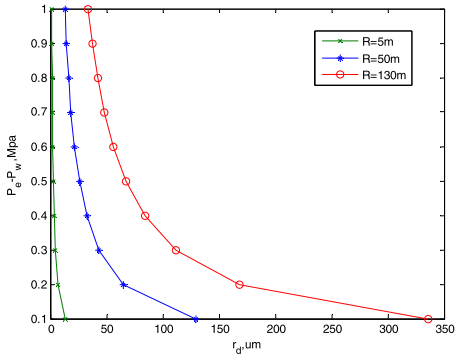

Table 2 Parameter values in a constant displacement pressure gradient

R, m	r_D, μm	J_k, %	E_D
5	6.465	94.18	0.937788
10	12.93	83.47	0.89356
15	19.395	60.36	0.836094
20	25.86	45.89	0.806094
25	32.325	36.21	0.782941
30	38.79	29.05	0.683835
35	45.255	24.33	0.653835
40	51.72	20.1	0.573835
45	58.185	18.63	0.423835

By using Eq. (10) gives:

$$r_D = \frac{0.2586R}{(P_e - P_w)_i}. \tag{23}$$

The Occurrence radius distribution curve in different places and pressure gradient can be achieved, see Fig. 3 and Fig. 4.

Assume that the displacement pressure gradient is 0.2 Mpa, and then parameter values are obtained: see Table 2, Fig. 5 and Fig. 6.

Figure 5 shows that the Percentage of water entries into rock pore decreased by occurrence radius, when the occurrence radius is small enough, the water can 100% enter the pore capillary.

Figure 6 shows: the oil displacement efficiency decreased by occurrence radius. When the occurrence radius is smaller than 25 μm, the oil displacement efficiency is over 80%,

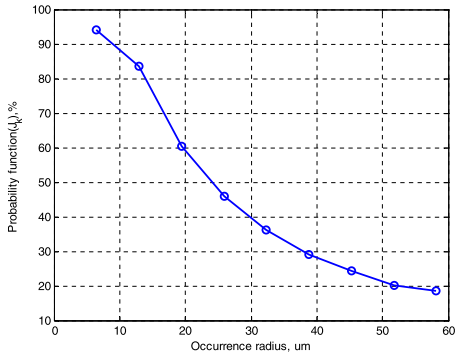

Figure 5 Percentage of water entries into pore capillary changed by occurrence radius

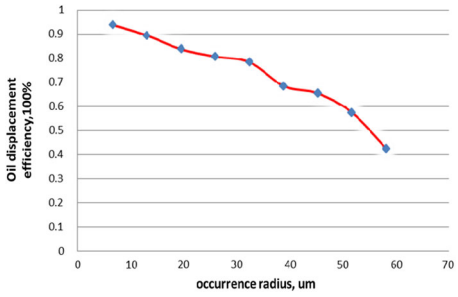

Figure 6 Oil displacement efficiency changed by the occurrence radius in GD7-42-J195TG block

and when $R = 5$ m, $r_D = 6.465\ \mu$m, the oil displacement efficiency is near to 0.937788 in the GD7-42-J195TG block. Hence, the oil displacement efficiency decreased by occurrence radius.

According to the definition of oil displacement efficiency, gives

$$E_D(r_D) = \frac{1 - s_{\text{or}} - s_{\text{wc}}}{1 - s_{\text{wc}}}. \tag{24}$$

When the displacing time and pressure gradient is big enough, the remaining oil saturation equals to the residual oil saturation, it is $s_{\text{or}} = s_o$, the oil displacement efficiency maximized.

Hence, the oil saturation in any place can be calculated

$$s_{\text{or}} = (1 - s_{\text{wc}})\big(1 - E_D(r_D)\big). \tag{25}$$

Here, statistics method is used to calculate the average oil saturation $\overline{s_o}$

$$\overline{s_o} = \frac{\sum_{r_D} \phi(r_D)(1 - s_{\text{wc}})(1 - E_D(r_D))}{m}. \tag{26}$$

Using Eq. (26) and data of Table 2, water saturation is achieved, $s_o(\Delta p = 0.2\ \text{Mpa}) = 0.22744$.

By using the same method, the oil saturation in different displacement rate (0.05 mL/min; 0.5 mL/min; 2 mL/min) in different rock sample-A7, B9, C112 can be achieved, see Table 3.

(3) *NMR experiment: verification and discussion*. By carrying Out Nuclear Magnetic Resonance experiments and using rock samples A7, B9, C12, T2 distribution curve Fig. 7, Fig. 8 and Fig. 9 and MRI Fig. 10, Fig. 11 and Fig. 12, oil saturation Table 4 are obtained.

Table 3 Theoretical calculating results of oil saturation

Sample	Remaining oil saturation, %		
	0.05 mL/min	0.5 mL/min	2 mL/min
A7	34.34	27.27	19.94
B9	34.28	26.32	20.19
C112	36.16	27.28	21.37

Figure 7 T2 distribution curve of sample A7 in different flow speed

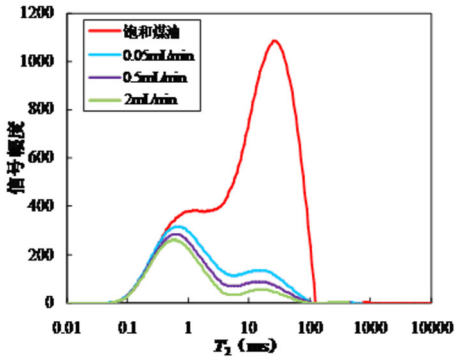

Figure 8 T2 distribution curve of sample B9 in different flow speed

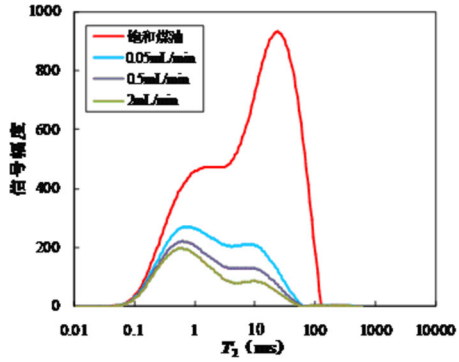

Figure 9 T2 distribution curve of sample C112 in different flow speed

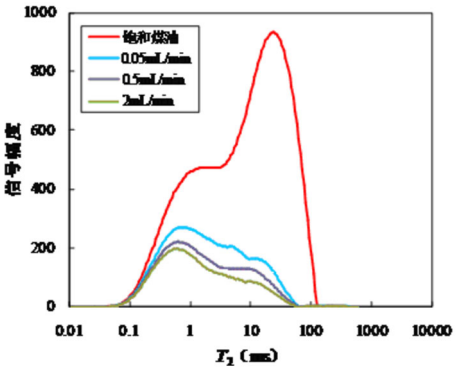

In Fig. 10, Fig. 11 and Fig. 12 the oil is red and the water is blue, separately. Figure 10, Fig. 11 and Fig. 12 show: the remaining oil saturation can be achieved and the residual mechanism can be concluded.

By analyzing the data in Table 3 and Table 4, Fig. 13 is obtained.

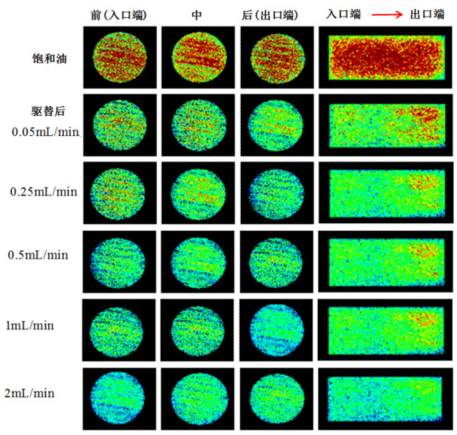

Figure 10 MRI of sample A7 in different flow speed

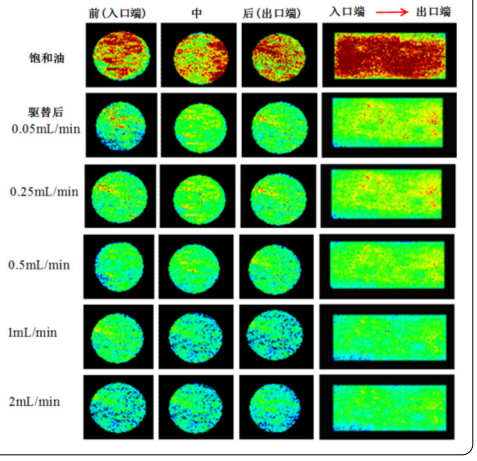

Figure 11 MRI of sample B9 in different flow speed

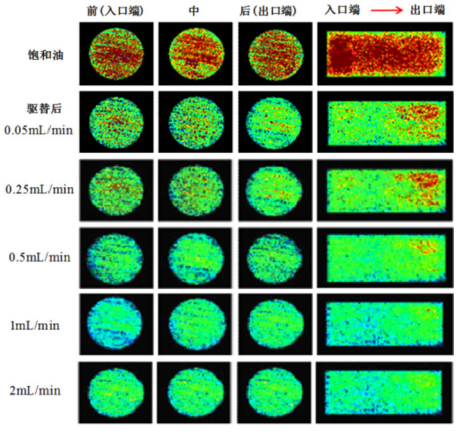

Figure 12 MRI of sample C112 in different flow speed

Figure 13 show that the theoretical calculating results of oil saturation is close to the experimental results. The oil saturation variance of sample-A7 is 2.116367, sample-B9 is 3.3992, and sample-C112 is 2.978333. Hence, new method can be used to guide the oilfield development.

Table 4 Remaining oil saturation with NMR experiment

Samples	Remaining oil saturation, %		
	0.05 mL/min	0.5 mL/min	2 mL/min
A7	33.13	26.34	21.45
B9	35.7	25.93	20.65
C12	35.21	25.13	20.27

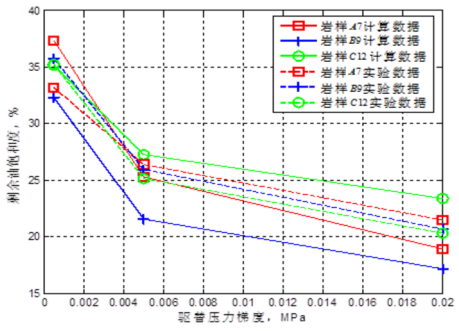

Figure 13 Comparison of remaining oil saturation from the prospective of theory and experiment

5 Conclusions

(1) Occurrence radius of remaining oil is decided by pressure gradient, wetting angle, well distance, the unit length, the bottom radius, the boundary distance and the interfacial tension, influencing the oil displacement efficiency, it collects micro factors and macro factor in a special way.

(2) MIP experiments data show that the distribution of pore radius is normal, and the probability expression can be worked out by numerical fitting method, and it can be used to calculate pore radius distributions of new blocks in the same oil reservoir.

(3) Not all of the injected water enters the capillary pores, the residual part, the discontinuous part and the possible formation pathway should be taken into consideration.

(4) The micro oil displacement efficiency decreased by occurrence radius.

(5) NMR experiments can be used to test the accuracy of the new method, and the experiments data of rock samples A7, B9, C12 show: the NMR experiments values (oil saturations) are in accordance with the values calculated by new method.

Acknowledgements

I always acknowledge reviewers and the associate editor and the support of Scientific Project of the Scientific Project of the vocational colleges teaching steering committee in ministry of education of China, No. 2018GGJCKT200 and the scientific project of Sichuan science and technology department, No. 2018CC0109.

Funding

Here, I offer my regards and blessings to the Scientific Project of the vocational colleges teaching steering committee in ministry of education of China and the and the scientific project of education department of Sichuan Province, helping me taking the MIP experiment and collecting the initial data here.

Abbreviations

MIP, Mercury intrusion porosimetry; NMR, Nuclear Magnetic Resonance; EOR, Enhanced oil recovery; $\overline{v}$, Flow speed, ml/min; K, Permeability, $\mu\mathbf{m}^2$; μ, Viscosity, $\mathbf{mpa}\cdot\mathbf{s}$; Δp, Pressure gradient, $\mathbf{Mpa}$; ∇, Nabla operator; R, Distance between the arbitrary point of formation and the production well, $\mathbf{m}$; r_e, Distance between the formation border and the production well, $\mathbf{m}$; r_w, Bottom radius, $\mathbf{m}$; p_e, Border formation pressure, $\mathbf{m}$; p_w, Bottom well pressure, $\mathbf{m}$; $p_{R+\delta_R}$, Formation pressure in position $R+\delta_R$, $\mathbf{Mpa}$; p_R, Formation pressure in position R, $\mathbf{Mpa}$; δ_R, Formation unit length, $\mathbf{m}$; σ, Interfacial tension, $\mathbf{N/m}$; r, Capillary radius, μm; θ, Wetting angle, °; r_D, Occurrence radius of remaining oil in capillary, μm; $\phi(r)$, Probability distribution of pore radius; $r_{\max}$, Capillary radius maximum, μm; $r_{\min}$, Capillary radius minimum, μm; $\bar{R}$, Average capillary radius, μm; σ_R, Standard deviation of pore radius; C, Fitting coefficient of pore radius probability distribution; $V(r_i)$, Capillary volume with radius r_i, $\mu\mathbf{m}^3$; r_i, Capillary radius (ith), μm; $E_{D1}(r_D)$, Displacement efficiency without considering the discontinuous characteristics, μm; q, Flow, $\mathbf{cm}^3\cdot\mathrm{min}^{-1}$; L, Capillary length, μm; $\eta(r,L)$, Fluid

conductivity, $\mathbf{ml} \cdot \mathrm{min}^{-1} \cdot \mathbf{Mpa}^{-1}$; $J(r_D)$, Probable function for injection water entering capillary; $E_D(r_D)$, Micro displacement efficiency considering the discontinuous characteristics, μm; $S_{\mathbf{or}}$, Micro residual oil saturation; $S_{\mathbf{wc}}$, Bound water saturation; $\overline{S_o}$, Average residual oil saturation.

Availability of data and materials
Fig. 1 in Sect. 3 is based on the MIP experiment data of SL oilfield in China (the initial data figure). Figure 6, Fig. 7 and Fig. 8 are MRI of samples of A7, B9 and C112 in different flow speed in SL oilfield (the initial data figure). Data sharing not applicable to this article as no datasets were generated or analyzed during the current study.

Competing interests
I declare that there is no competing interest.

Authors' contributions
The main idea of this paper was proposed by HL, and the author prepared the manuscript initially and performed all the steps of the proofs in this research. The author read and approved the final manuscript.

Authors' information
Haohan Liu (1985-08), Ph.D. of oil and gas development engineering, vice professor, post-doctor, engaged in oil and gas development for 8 years, interested in optimization and statistics theory and application.

Publisher's Note

Received: 3 September 2018 Accepted: 10 April 2019 Published online: 29 April 2019

References

1. Jadhunandan PP, Morrow NR. Effect of wettability on waterflood recovery for crude-oil/brine/rock systems. SPE Reserv Eng. 1995;10(1):40–6.
2. Morrow NR. Wettability and its effect on oil recovery. J Pet Technol. 1990;24(12):1476–84.
3. Li P. Brief introduction to low-permeability oilfield development. Petr Geol Oilfield Dev Daqing. 1997;03:36–40 (in Chinese).
4. He W, Yang Y et al. Expertimental study on waterflooding in ultra-low permeability reservoirs. Lithol Reserv. 2010;04:109–11 115 (in Chinese).
5. Wang Y, Ying B. Relationship between reservoir pore structure and displacement efficiency. Henan Petr. 1999;13(1):23–5 (in Chinese).
6. Cai Z. The study on the relationship between pore structure and displacement efficiency. Petr Explor Dev. 2000;06:45–9 (in Chinese).
7. Sheng P. Basic research on enhancing oil recovery of matured oil fields. China Basic Sci. 2003;02:39–42 (in Chinese).
8. Chen T, Lin F. Impact of salinity on warm water-based mineable oil sands processing. Can J Chem Eng. 2017;95(2):181–9.
9. Yu Q. Drive curves and decline curves for water drive field. Petr Explor Dev. 1995;01:39–42 (in Chinese).
10. Lu W. A study on displacement characteristics of SZ36-1 oil field. China Offshore Oil and Gas (Geology). 2003;03:34–7 (in Chinese).
11. Yan Z. Discussion on prediction of waterflooding displacement efficiency with field production data. Pet Geol Recovery Effic. 2010;03:99–101 (in Chinese).
12. Long J. The research of S oilfield extra high water cut period to displacement characteristics affection. North East Petroleum University. 2014;20–28.
13. Fu X, Sun W. Study of microscopic oil–water displacement mechanism of low-permeability reservoir. Xinjiang Petrol Geol. 2005;26(6):681–3.
14. Li F, Luo Y, Hu P, Yan X. Intrinsic viscosity, rheological property, and oil displacement of hydrophobically associating fluorinated polyacrylamide. J Appl Polym Sci 2016;134(14).
15. Soares Silva R, Lyra PRM et al. A higher resolution edge-based finite volume method for the simulation of the oil–water displacement in heterogeneous and anisotropic porous media using a modified IMPES method. Int J Numer Methods Fluids. 2016;82(12).
16. Zheng X, Mahabadi N. Effect of capillary and viscous force on CO_2 saturation and invasion pattern in the microfluidic chip. J Geophys Res, Solid Earth. 2017;122(3).
17. Kang DH, Yun TS. Minimized capillary end effect during CO_2 displacement in 2-d micromodel by manipulating capillary pressure at the outlet boundary in lattice Boltzmann method. Water Resour Res. 2018;54(6):895–915.
18. Liu HH. Study on remaining oil droplet dynamic conditions and water flood efficiency changing mechanisms in the ultra-high water cut period. Southwest Petroleum University. 2013;9–11 (in Chinese).
19. Liu HH. Modified theoretical expression of water saturation in oil–water fluid flow area. Open Petrol Eng J. 2013;6(1):76–8.
20. Yue P, Xie Z, Huang S, Liang S, Chen X. The application of N2 huff and puff for IOR in fracture-vuggy carbonate reservoir. Fuel. 2018;234:1507–17.
21. Liu ZB, Liu HH. An effective method to predict oil recovery in high water cut stage. J Hydrodyn, B. 2016;27(6):988–95.
22. Yue P, Xie Z, Liu H, Chen X, Guo Z. Application of water injection curves for the dynamic analysis of fractured-vuggy carbonate reservoirs. J Pet Sci Eng. 2018;169:220–9.
23. Yue P, Chen X, Liu H, Jia H. The critical parameters of a horizontal well influenced by a semi-permeable barrier considering thickness in a bottom water reservoir. J Pet Sci Eng. 2015;129:88–96.
24. Liu ZB, Liu HH. Multi-factors prediction of water flooding efficiency based on time-varying system. Commun Stat, Theory Methods. 2016;45(20):5873–83.